Rabi oscillation generation in the microring resonator system with double-series ring resonators*

Ahmad Fakhrurrazi Ahmad Noorden¹, Kashif Chaudhary¹, Mahdi Bahadoran¹, Muhammad Safwan Aziz¹, Muhammad Arif Jalil¹, Ong Chee Tiong², Jalil Ali¹, and Preecha Yupapin³**

1. Institute of Advance Photonics Science, Nanotechnology Research Alliance, Universiti Teknologi Malaysia, Johor Bahru 81300, Malaysia

2. Department of Mathematics, Universiti Teknologi Malaysia, Johor Bahru 81310, Malaysia

3. Advanced Studies Center, Faculty of Science, King Mongkut's Institute of Technology Ladkrabang, Bangkok 10520, Thailand

In this paper, a microring resonator (MRR) system using double-series ring resonators is proposed to generate and investigate the Rabi oscillations. The system is made up of silicon-on-insulator and attached to bus waveguide which is used as propagation and oscillation medium. The scattering matrix method is employed to determine the output signal intensity which acts as the input source between two-level Rabi oscillation states, where the increase of Rabi oscillation frequency with time is obtained at the resonant state. The population probability of the excited state is higher and unstable at the optical resonant state due to the nonlinear spontaneous emission process. The enhanced spontaneous emission can be managed by the atom (photon) excitation, which can be useful for atomic related sensors and single-photon source applications.

Document code: A **Article ID:** 1673-1905(2015)05-0342-6

DOI 10.1007/s11801-015-5090-2

Optical microring resonator (MRR) has emerged as a potential photonic structure in integrated technology with low power consumption[1]. MRR contributes in various technological applications, such as optical sensors[2], optical amplification[3], polarization conversion[4], optofluidic devices[5], optical spin generators[6], frequency shifters[7] and on-chip spectrometry bio-analysis[8]. In quantum, the interaction between atoms and electromagnetic field is described precisely by the energy state transition as interaction phenomenon occurs in small distance with short time.

The probability of atom transition between two energy levels is used to explain the interaction between electromagnetic field and atoms. Based on the perturbation theory, the atomic state population remains constant, as the probability amplitude of an atom transiting to other energy states is small. However, in presence of strong light field, the atomic population increases in higher energy level[9]. The probability of atom transition is found in form of oscillation against time which shows that the atom could be in ground or higher energy level, and such oscillations are known as Rabi oscillation[10]. The energy states for a system can be analyzed using the Hamiltonian of time-dependent Schrodinger equation for the light-atom interaction.

In this paper, a theoretical formulation for the optical bright soliton pulse propagation within the nonlinear silicon-on-insulator (SOI) double-series microring resonator (DSMRR) system is presented based on optical transfer function[11] and scattering matrix method[12]. The SOI shows the nonlinear optical properties at various wavelengths, which provides strong light confinement[13] and is suitable for high-speed passive-waveguide applications. The Rabi oscillation at the through port of DSMRR system is described by the Hamiltonian, which represents the atoms with ambient surrounding as an unperturbed condition and the atoms interacting with optical bright soliton beam as a perturbed condition. The Rabi frequency equations for the interaction between atom and light within the DSMRR system are obtained by the analytical derivation of two-level atom approximation. The output intensity of the DSMRR and the Rabi oscillation are analyzed and investigated for probability of finding the particles in excited states. The potential of Rabi frequency and oscillation in a nonlinear microring circuit for switching and sensing applications is also discussed.

The two-level atom is used to manipulate light as a particle which propagates in a nonlinear DSMRR, where the ground and excited states of the atom during interac-

tion are given by $\left|\psi_{\mathrm{g}}\right\rangle$ and $\left|\psi_{\mathrm{e}}\right\rangle$ with energy eigenvalues of E_{g} and E_{e}, respectively. The energy difference related to the transition energy of atom is given as $\hbar\omega_0 = E_{\mathrm{g}} - E_{\mathrm{e}}$ with atomic transition angular frequency of ω_0. The Hamiltonian of two-level system is given as[9,10]

$$\hat{H}\psi(r,t) = (\hat{H}_0 + \hat{H}_{\mathrm{int}})\psi(r,t), \tag{1}$$

where $\hat{H}_0$ shows the unperturbed Hamiltonian operator, and $\hat{H}_{\mathrm{int}}$ is the perturbed Hamiltonian operator. The atom Hamiltonian and the field Hamiltonian both contribute to the unperturbed Hamiltonian as

$$\hat{H}_0 = \hat{H}_{\mathrm{a}} + \hat{H}_{\mathrm{f}}, \tag{2}$$

where the atomic Hamiltonian is

$$\hat{H}_{\mathrm{a}} = \frac{P^2}{2m} + \hbar\omega_0 a^\dagger a, \tag{3}$$

and the field Hamiltonian is given as

$$\hat{H}_{\mathrm{f}} = \hbar\omega_0 a^\dagger a, \tag{4}$$

where P is the center-of-mass momentum operator, m is the mass of atom, $\hbar\omega_0$ is the energy of photon, and $a^\dagger$ and a are the atomic ladder operators as illustrated in Fig.1.
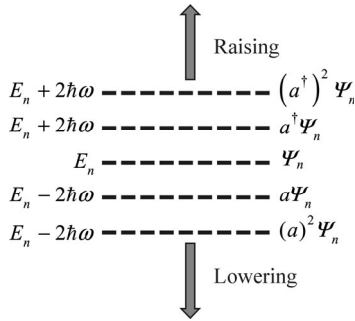

Fig.1 Equal spaced ladder energy level generated by multiple action of ladder operator to the state with energy of E_n

The interaction Hamiltonian is given by $\hat{H}_{\mathrm{int}}$ in Eq.(1), which describes the coupling of the electromagnetic field to atom, and the electric dipole moment operator d is given in

$$\hat{H}_{\mathrm{int}} = -d \cdot E(t). \tag{5}$$

At this point, a spatially uniform dipole approximation is considered. The atomic behavior is described by the general state which can be expressed as a linear combination. The general solution of time-dependent Schrodinger equation (TDSE) state is equal to the sum of the states in the system, which is given as

$$\psi(r,t) = \sum_i c_i(t)\psi_i(r)\exp(-iE_i t/\hbar). \tag{6}$$

The subscript i indicates each Eigen state which exists in the system. The TDSE solution is represented to the ground state and the excited state for a two-level energy system as

$$\psi(r,t) = c_{\mathrm{g}}(t)\psi_{\mathrm{g}}(r)\exp(-iE_{\mathrm{g}}t/\hbar) +$$
$$c_{\mathrm{e}}(t)\psi_{\mathrm{e}}(r)\exp(-iE_{\mathrm{e}}t/\hbar), \tag{7}$$

where $c_{\mathrm{g}}(t)$ and $c_{\mathrm{e}}(t)$ are the amplitudes of the wavefunction for the two-level energy system, which indicate ground state ψ_{g} and excited state ψ_{e}, respectively. The states $\psi_{\mathrm{g}}(r)$ and $\psi_{\mathrm{e}}(r)$ are the position-space wave functions which satisfy the orthonormal states as given in

$$\langle\psi_{\mathrm{g}}|\psi_{\mathrm{e}}\rangle = \delta_{\mathrm{ge}}, \tag{8}$$

where δ_{ge} is the Kronecker delta function.

By substituting the wave functions given in Eq.(7) into the Hamiltonian Eq.(1), with consideration of the rotating wave approximation, and neglecting the rapidly oscillating term, $\omega - \omega_0 \ll \omega$, the differential forms of $c_{\mathrm{g}}(t)$ and $c_{\mathrm{e}}(t)$ can be determined as[9]

$$\dot{c}_{\mathrm{g}} = i\Omega_{\mathrm{R}}^* c_{\mathrm{e}} e^{i\Delta t}, \tag{9}$$

$$\dot{c}_{\mathrm{e}} = i\Omega_{\mathrm{R}} c_{\mathrm{g}} e^{-i\Delta t}, \tag{10}$$

where $\Delta \equiv \omega - \omega_0$ is the detuning parameter, and Ω_{R} is the Rabi frequency which represents the frequency of oscillation for atomic transition in light field. Eqs.(9) and (10) are well-known mathematical representation of Rabi oscillation between the ground and the excited states for a two-level system. From the trial solution of $c_{\mathrm{e}}(t) = e^{i\lambda t}$, and by considering the initial conditions of $c_{\mathrm{g}}(0) = 1$ and $c_{\mathrm{e}}(0) = 0$, the normalized probabilities to find atom in ground and excited states are given as

$$P_{\mathrm{g}}(t) = |c_{\mathrm{g}}(t)|^2 = \cos^2(\Omega_{\mathrm{R}}t/2), \tag{11}$$

$$P_{\mathrm{e}}(t) = |c_{\mathrm{e}}(t)|^2 = \sin^2(\Omega_{\mathrm{R}}t/2), \tag{12}$$

where $\Omega_{\mathrm{R}} = |E_0\mu_{12}/\hbar|$ is the total Rabi frequency[10], which is related to the electric field equation of $E(r) \approx E_0(z) = \vartheta A(z)e^{i\beta_0 z}$ with $\vartheta = (\mu_0/\varepsilon_0)^{1/4}(2n_0)^{1/2}$. μ_0 and ε_0 are the permeability and permittivity in vacuum, respectively. n_0 is the linear refractive index, $\beta_0 = \omega n_0/c$ is the propagation constant, c is the speed of light, and $A(z)$ is the complex amplitude. For defining the impact of two-photon absorption (TPA) and free-carrier effect of optical wave[14,15], the evolution of electric field associated with this optical wave is described by a nonlinear differential equation as

$$\partial A/\partial z = -\alpha A/2 + i\gamma|A|^2 A, \tag{13}$$

where α is the linear loss, and $\gamma = kn_2$ represents the Kerr effect, where k and n_2 are the wave number and nonlinear refractive index, respectively. The solution of Eq.(13) is given as

$$A(r,t) = \sqrt{I(t)}\exp[i\phi(z)], \tag{14}$$

and the required result in term of intensity[10] can be expressed as

$$I = \frac{1}{2}c\varepsilon_0 nE^2. \tag{15}$$

The schematic diagram of a nonlinear DSMRR system with the notation is shown in Fig.2. The optical bright soliton pulse with angular frequency of ω_0 used for the optical input pulse of the DSMRR waveguide[6,16] is given as

$$E_{in}(t) = A_0 \text{sech}\left(\frac{T}{T_0}\right)\exp\left(\frac{x}{2L_D} - i\omega_0 t\right), \qquad (16)$$

where E_{in} represents the electric field of optical bright soliton, and A_0 depicts the optical field amplitude with the propagation length x. The pulse propagation time is $T = t - \beta_1 x$, and T_0 is the initial propagation time. β_1 and β_2 are the coefficients of the linear and the second-order terms of Taylor expansion of propagation. $L_D = T_0/|\beta_2|$ is the dispersion length of the soliton pulse, and t is the phase shift. Fig.2 illustrates the microring resonator configuration which consists of two MRRs and one bus planar waveguide with optical bright soliton propagation along straight SOI waveguide coupled laterally to a ring with radius of R.
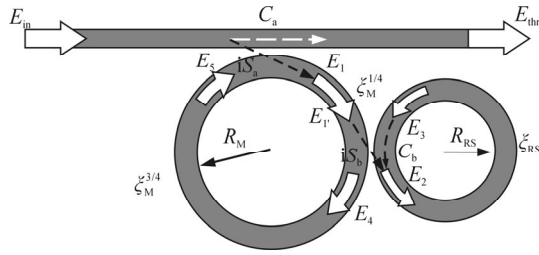

Fig.2 The schematic diagram of DSMRR system (E_i: optical electric fields; R: radius of ring; ξ: single-pass phase shift)

The radii of main microring (R_M) and the right-sided microring (R_{RS}) are 5 μm and 2 μm, respectively. The dotted and dash arrows represent the cross-coupling coefficients iS between two waveguides and self-coupling coefficients C through a waveguide, which can be described as

$$iS_a = i\sqrt{\kappa_a}\sqrt{1-\gamma_a}, \quad iS_b = i\sqrt{\kappa_b}\sqrt{1-\gamma_b}, \qquad (17)$$

$$C_a = \sqrt{\kappa_a - 1}\sqrt{1-\gamma_a}, \quad C_b = \sqrt{\kappa_b - 1}\sqrt{1-\gamma_b}, \qquad (18)$$

where κ_a and κ_b are the coupling coefficients for coupling regions 1 and 2 as illustrated in Fig.3, respectively, and γ is the propagation loss as the pulse travels within the waveguide materials. The electric fields on both sides of the point coupler satisfy the following relations as[17]

$$E_1 = iS_a E_{in} + C_a E_5, \qquad (19)$$

$$E_{1'} = E_1 \xi_M^{1/4}, \qquad (20)$$

$$E_2 = iS_b E_{1'} + C_b E_3, \qquad (21)$$

$$E_3 = E_2 \xi_{RS}, \qquad (22)$$

$$E_4 = iS_b E_3 + C_b E_{1'}, \qquad (23)$$

$$E_5 = E_4 \xi_M^{3/4}, \qquad (24)$$

$$E_{thr} = iS_a E_5 + C_a E_{in}, \qquad (25)$$

where $\xi_M^{1/4}$, $\xi_M^{3/4}$ and ξ_{RS} are the single-pass phase shifts as the electric field propagates in bending waveguide, which are given as[18]

$$\xi_M^{1/4} = \exp\left[\left(\frac{\alpha}{2}L_M\right)(1/4) - ik_n(L_M/4)\right], \qquad (26)$$

$$\xi_M^{3/4} = \exp\left[\left(\frac{\alpha}{2}L_M\right)(3/4) - ik_n(3L_M/4)\right], \qquad (27)$$

$$\xi_{RS} = \exp\left[\left(\frac{\alpha}{2}L_{RS}\right) - ik_n L_{RS}\right], \qquad (28)$$

where α is the attenuation constant, and k_n is wave-vector with corresponding refractive index of the system[19].

Thus the ratio of the output electric field at through port E_{thr} to input electric field E_{in} is given as

$$\frac{E_{thr}}{E_{in}} = \frac{C_1^2 - \dfrac{\xi_M(\xi_{RS} - C_2)}{1 - \xi_{RS}C_2}}{1 + \left[\dfrac{\xi_M(\xi_{RS} - C_2)}{1 - \xi_{RS}C_2}\right]C_1}. \qquad (29)$$

The through port electric field E_{thr} of the MRR system is proportional to the output intensity as shown in Eq.(15).
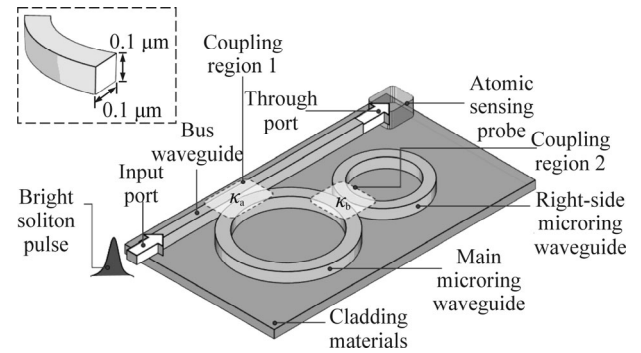

Fig.3 The planar SOI DSMRR configuration and the cross-sectional area shown in the inset

The manipulation of the Rabi oscillation is performed using bright soliton pulse as the input source for MRR system. The MRR system consists of two coupling regions between bus waveguide and main microring waveguide and between main microring and right-sided microring waveguide as shown in Fig.3. The radius of right-side ring is smaller than that of main ring to avoid another coupling with the bus waveguide. As the evanescent field of bright soliton pulses is coupled to the ring waveguide, the intensity of coupled field is enhanced as it propagates within the SOI MRR waveguide due to nonlinear effects. The output light is used as the optical radiation source for the Rabi oscillation as shown in Fig.3, which can be used as the atomic sensing probe.

In this paper, the calculation is performed for an SOI DSMRR with radii of main and right-sided rings of R_M=5 μm and R_{RS}=2 μm, respectively, center wavelength of λ=1 550 nm, effective refractive index of n_0=3.484, attenuation constant of α=1 dB/cm^2 and refractive index of n_2=6×10^{-18} m^2/W[14]. The transmission signal of the MRR system is investigated, and the transmitted output intensities (at through port) versus the soliton input intensity with different coupling coefficients of the system are shown in Fig.4(a). Fig.4(b)–(d) are the enlargements of Fig.4(a) for each coupling coefficient, which shows the bistability and hysteresis loop of the transmission output signal due to the nonlinear effect.

The arrows in Fig.4(b)–(d) indicate the switching power working principles for ON and OFF operation. As shown in Fig.4(a), the optical bistability effect[20,21] initiates at 8.68 GW/cm^2, 12.32 GW/cm^2 and 15.01 GW/cm^2 and ends at 10.15 GW/cm^2, 13.94 GW/cm^2 and 21.95 GW/cm^2 for the coupling coefficients of 0.4, 0.5 and 0.6, respectively. The increase of coupling coefficient widens the range of the bistability signal with respect to the input intensity. The transmission signal shows that the increase of coupling coefficient causes the weaker switching as the area hysteresis loop of the signal is reduced. The bistablity DSMRR system can also be used as a flip-flop. The white-dots on the hysteresis loop of two stable states indicate the positions of threshold switching power with respect to input signal, which can act as the trigger points for flip-flop operation[22].

(a)

(b) κ_3=0.4
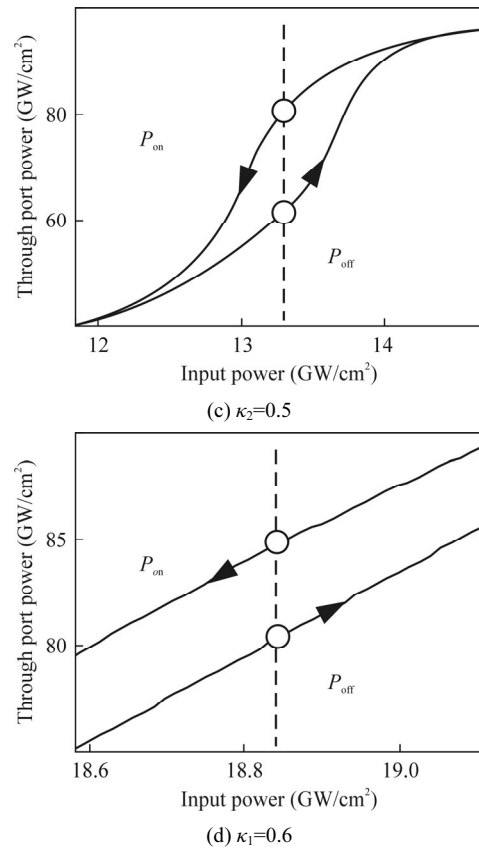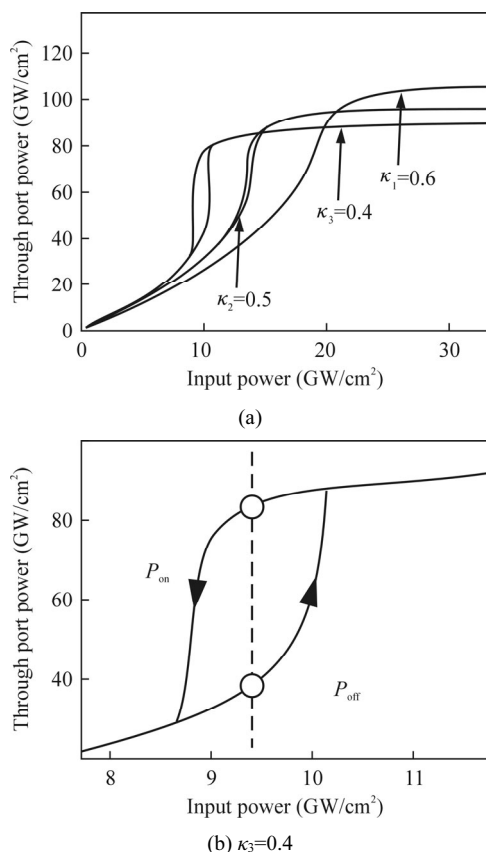

(c) κ_2=0.5

(d) κ_1=0.6

Fig.4 (a) Bistability hysteresis curves of through port transmission signal and (b)–(d) the enlargements for different coupling coefficients
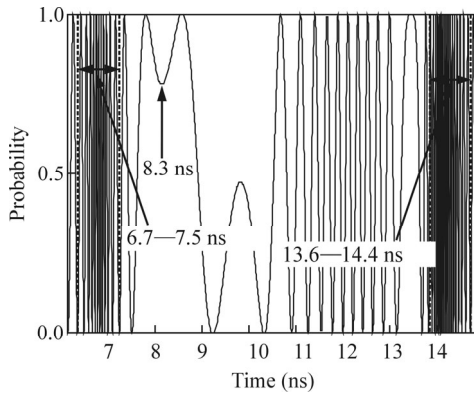
The probabilities of finding atoms in the excited and ground states at the through port are illustrated in Fig.5. Initially, the atoms are shifted to the excited state from the ground state due to interaction with optical soliton pulse and cause the increase of frequency with respect to the time as shown in Fig.5(a). As the intensity increases at through port, the transition probability becomes unstable due to nonlinear optical resonance effect in the DSMRR system as shown in Fig.5(b) and (c).

The high frequencies of the Rabi oscillations are observed in the ranges from 6.7 ns to 7.5 ns and from 13.6 ns to 14.4 ns, where the radiation intensity at the through port is also higher. The nonlinear resonant intensity (bistability) is obtained between 7.5 ns and 13.6 ns as shown in Fig.5(b) and (c), which produces an unstable (damping) oscillation with population probabilities of 0.8 and 0.2 at 8.3 ns for excited and ground states, respectively. Moreover, the decreases of frequency and amplitude of Rabi oscillations are observed at 9.7 ns, where the population probabilities at excited and ground energy states are 0.6 and 0.4, respectively. The atom stays active in the middle of both states and delays the oscillation, till it absorbs the photon from the pulse at through port before it de-excites and generates Rabi oscillation. The relation of the normalized transmission intensity at the through port with the Rabi frequency in gigahertz is calculated and shown in Fig.6. The increase of the optical
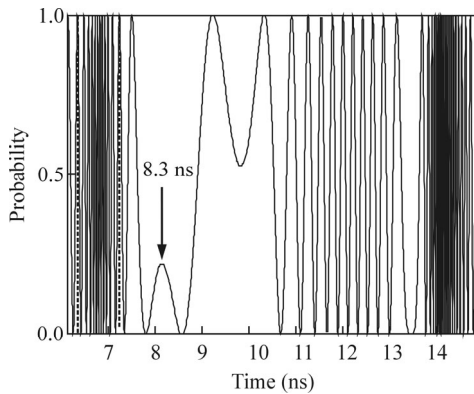
intensity contributes to the enhancement of Rabi frequency.
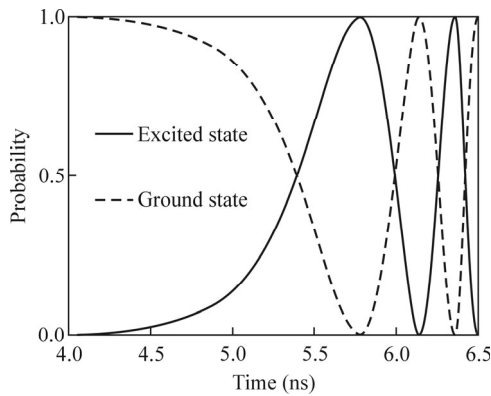
(a) For excited state and ground state with time range from 4 ns to 6.5 ns

(b) For excited state with time range from 6.5 ns to 14.5 ns

(c) For ground state with time range from 6.5 ns to 14.5 ns

Fig.5 Probabilities of finding atoms in the ground and excited states

The Rabi frequency becomes unstable due to the resonance effect of pulse at through port. For instance, 86% normalized intensity at the through port is obtained at 10.6 ns as shown in Fig.7. The Rabi frequency begins to decline when the intensity of the system is increased to 99%. The damping of the Rabi oscillation provides the unusual behavior of the atoms between ground and excited states as shown in Fig.7.

The dashed lines in inset of Fig.7 represent the time interval from 7.75 ns to 13.28 ns for optical resonance effect within the DSMRR system. The intensity is de-

creased as pulses propagate for 10 000 round trips in which it reaches the resonance state due to the nonlinear effect of the system. Due to the decrease of intensity at through port, the Rabi frequency is unstable, which causes the random spontaneous emission generated by the excited atoms. At the excited state, atoms undergo the near-elastics collision due to conservation of energy, and the phase of the wave-function is randomly changed. The change of phase causes the damping of oscillation which depends on the phase coherence. The random spontaneous emission causes disturbance on the coherence phase of optical resonance pulses, and hence reduces the oscillation frequency.
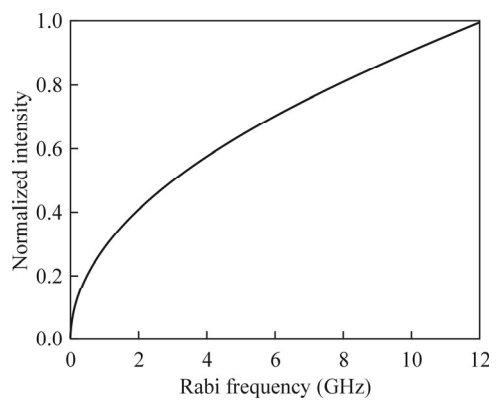

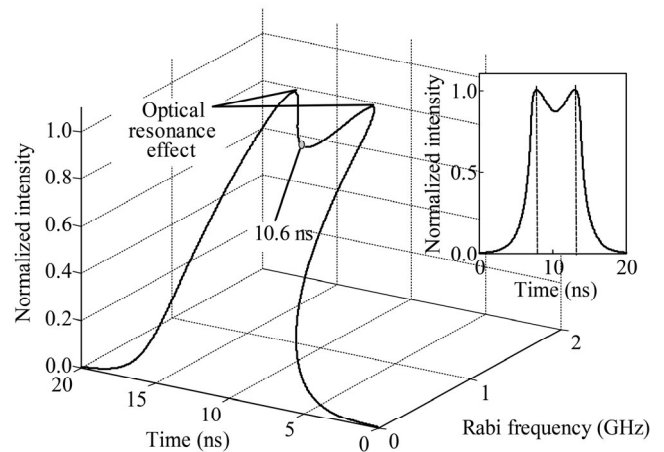**Fig.6 Relation between output intensity and Rabi frequency at the through port**

Fig.7 The Rabi frequency behavior with respect to time and the through port intensity

When the optical pulse intensity is high, the spontaneous emission can be negligible, while when the intensity is reduced, the spontaneous emission must be considered. This relation between the spontaneous emission rate and the light intensity is known as Purcell effect. The enhancement of the spontaneous emission by excited atom becomes one of the possible ways for atomic sensors[23] and single-photon sources[24] as the process can be controlled by manipulating the quality factor of microring resonator.

A DSMRR system is proposed to generate and investigate the Rabi oscillations. The hysteresis loop is achieved from the proposed configuration, and it is independent of coupling coefficients κ_i of the system. The numerical simulations reveal that the atomic transitions in core medium depend on the resonance intensity which will influence the Rabi frequency. The probability of finding the atom at the excited state is higher in the resonance condition. The Rabi oscillation frequency is increased with time before it reaches the resonance state. The damping in the oscillations is observed in resonance state due to high population in excited state in time range from 7.75 ns to 13.28 ns. In the resonance state, the SDMRR system generates the unstable oscillation for a period of time called as resonance time. The calculation of the Rabi oscillation can be useful for applications, and more complicated circuits, such as add-drop filter, polarization maintaining and absorption reducing (PANDA) ring resonator and cascaded system, can be used as the atomic sensor.

Acknowledgments

References

[1] Chremmos I., Uzunoglu N. K. and Schwelb O., Photonic Microresonator Research and Applications, New York: Springer, 2010.

[2] Sumetsky M., Windeler R. S., Dulashko Y. and Fan X., Optics Express **15**, 14376 (2007).

[3] Rabus D. G., Bian Z. X. and Shakouri A., IEEE Journal of Selected Topics in Quantum Electronics **13**, 1249 (2007).

[4] Fietz C. and Shvets G., Optics Letters **32**, 1683 (2007).

[5] White I. M., Gohring J., Sun Y., Yang G., Lacey S. and Fan X., Applied Physics Letters **91**, 2411041 (2007).

[6] Glomglome S., Srithanachai I., Teeka C., Mitatha S., Niemcharoen S. and Yupapin P.P., Optics and Laser Technology **44**, 1294 (2012).

[7] Fan G, Li Y, Hu C, Lei L, Zhao D, Li H and Zhen Z., Optics & Laser Technology **63**, 62 (2014).

[8] Nitkowski A., Baeumner A. and Lipson M., Biomedical Optics Express **2**, 271 (2011).

[9] Gerry C. and Knight P., Introductory Quantum Optics, Cambridge: Cambridge University Press, 2005.

[10] Fox M., Quantum Optics: An Introduction, New York: Oxford University Press, 2006.

[11] Ma C. S., Wang X. Y., Li D. L. and Qin Z. K., Optics and Laser Technology **39**, 1183 (2007).

[12] Shih C. T. and Chao S., Optics Express **17**, 7756 (2009).

[13] Ciminelli C., Dell'Olio F., Conteduca D., Campanella C. M. and Armenise M. N., Optics and Laser Technology **59**, 60 (2014).

[14] Rukhlenko I. D., Premaratne M. and Agrawal G. P., Optics Letters **35**, 55 (2010).

[15] Eason R. W. and Miller A., Nonlinear Optics in Signal Processing, Springer, 1993.

[16] Yupapin P. P. and Pornsuwancharoen N., IEEE Photonics Technology Letters **21**, 404 (2009).

[17] Phatharaworamet T., Teeka C., Jomtarak R., Mitatha S. and Yupapin P. P., Journal of Lightwave Technology **28**, 2804 (2010).

[18] Heebner J., Grover R., Ibrahim T. and Ibrahim T. A., Optical Microresonators: Theory, Fabrication, and Applications, London: Springer, 2008.

[19] Manjunatha K. B., Dileep R., Umesh G. and Bhat B. R., Optics and Laser Technology **52**, 103 (2013).

[20] Bahadoran M., Ali J. and Yupapin P. P., Applied Optics **52**, 2866 (2013).

[21] Bahadoran M., Ali J. and Yupapin P. P., IEEE Photonics Technology Letters **25**, 1470 (2013).

[22] Maywar D. N., Agrawal G. P. and Nakano Y., Journal of the Optical Society of America B: Optical Physics **18**, 1003 (2001).

[23] Hogan J. M., Johnson D. M. S., Dickerson S., Kovachy T., Sugarbaker A., Chiow S. W., Graham P. W., Kasevich M. A., Saif B., Rajendran S., Bouyer P., Seery B. D., Feinberg L. and Keski-Kuha R., General Relativity and Gravitation **43**, 1953 (2011).

[24] Vahala K. J., Nature **424**, 839 (2003).